Journal of Critical Reviews

ISSN- 2394-5125 Vol 7, Issue 1, 2020

Metallurgical and Mechanical Fatigue Behavior of Al 6061-T6 Subjected to Deep Cryogenic Treatment by using Cryogenic chamber

M.Bala Theja[1], D.Naveen Kumar[2] , K.Hema Chandra Reddy[3]

[1]Assistant Professor, Department of mechanical Engineering,SVR Engineering college,Nandyal, A.P., India

[2] Assistant Professor, Vathsalya Institute of Science and Technology (VIST), Yadadri Bhongir District,(T.S), India

[3] Professor, Department of mechanical Engineering, JNTUA college of Engineering, Ananthapuramu,A.P.,

[1]balathejaphd@gmail.com

Article History: Received : 29.06.2019 Review: 12.09.2019 Accepted: 28.09.2019 Published: 29.01.2020

ABSTRACT:

The impact of Deep cryogenic treatment (DCT) on the metallurgical and mechanical properties of Al6061-T6 is examined in the present work. The combination was subjected to Deep CT at - 196 ºC for 36 h. Mechanical tests, for example, Brinell hardness test, ductile, and weakness tests were performed on both local and treated examples. It was watched that the mechanical properties, for example, hardness, yield quality, and extreme rigidity expanded by around 41, 27, and 13%, separately, for the treated example. The treated amalgam was portrayed by utilizing the procedures, for example, optical microscopy, vitality dispersive x-beam spectroscopy (EDS), and to watch the adjustments in the metallurgical highlights. SEM-EDS comes about show precipitation, better dissemination of second-stage particles, and higher separation thickness in the regarded compound when contrasted with the untreated composite. The treatment confers enhanced hardness and quality to the compound because of precipitation solidifying and high separation thickness. Break morphologies of the treated and the local examples were portrayed by utilizing examining electron microscopy and it was watched that the striations were denser in the treated example supporting the higher weariness quality.

Keywords Al6061, fatigue, microstructure, shallow cryogenic treatment, tensile strength

1. INTRODUCTION

Aluminum and its amalgams are utilized as a part of an extensive variety of utilizations, from bundling to aviation businesses because of their high specific quality, crack quality, and erosion protection (Ref 1). Al composites with high quality to weight proportion give better mechanical properties as thought about than steels and can work under serious exhaustion situations. Subsequently they keep up pre-distinction as key auxiliary materials in airplane industry. This has prompted constant advancements in thermo mechanical handling of light metals and amalgams for enhancing their basic properties. 6000 arrangement aluminum compounds consti-tute aluminum, copper, zinc, and magnesium making it the most grounded of all the aluminum fashioned composites. Among 6000 arrangement aluminum compounds, 6061 is broadly utilized as a part of flying machine and arms enterprises in light of its prevalent quality (Ref 2). As a rule, the mechanical properties of 6061 amalgam are enhanced by diminishing its iron and silicon substance, and changing extinguish ing and maturing conditions (Ref 3). It shows great harm resilience and high protection from weariness split engendering in T6 matured condition (Ref 4).

Cryogenic treatment (CT) is widely used to improve the mechanical properties of metals and their alloys due to the phase transformations occurring in the alloy, especially for steels. Although the first atSEMpt to perform sub-zero treatments was investigated at the beginning of the 20th century, the actual interest on CT has developed during the last few decades (Ref The basic CT process consists of gradual cooling of the specimen until the defined SEMperature (normally below 0 °C), holding it for a stipulated time (freezing time) and then progressively leading it back to the room temperature. CTs are classified according to the minimum Temperature achieved during the process. In Shallow Cryogenic Treatments (DCT), the specimens are cooled down to —80 °C, while in deep cryogenic treatments (DCT) much lower Temperature are reached by using liquid nitrogen (—196 °C) or liquid helium (—269 °C) as cooling agents (Ref 5, 6).

Literature reports improvement in mechanical properties of DC-treated magnesium-based alloys. Liu et al. (Ref 7) have reported that the structure of AZ91 Mg alloy changed from disordered solid solution to ordered solid solution upon DCT. DCT induced the precipitation of second-phase particles, which contributes for strengthening as shown in their work. Similarly, Chen et al. (Ref 8) studied the effect of CT on the residual stress and mechanical properties of an aerospace aluminum alloy. It was observed in their work that DCT reduced the residual stress by up to 9 ksi in the parent metal with the improvement in stress corrosion cracking resistance of the alloy. Also, very small increase in microhardness, fatigue, and tensile properties were observed for the DCT alloy. A slight increase in strength and toughness, while a slight decrease in hardness was reported for the DCT-treated Al 6061 alloy with the soaking time varying between 2 and 48 h (Ref 5). Baldissera and Delprete (Ref 6) present a review on CTs of several alloys such as tool steel and aluminum. The phase transformation and evolution of precipitates in the ferrous metals and alloys subjected to CT contribute to the improved strength, wear resistance, and corrosion resistance as reported in the literature.

DCT in aluminum alloys result in fine grain size, optimum dispersion of second-phase elements, and high toughness (Ref

8). Most aluminum composites display changes in their microstruc-ture and mechanical properties when they are subjected to below zero Tem (Ref 9-11). The expansion in yield and rigid qualities however diminish in extension has been accounted for the Al compound (Ref 12, 13). The significant change in exhaustion life of ultrafine-grained Al 6061 T6 subjected to DCT has been accounted for in the writing (Ref 8, 10). Zhang et al. (Ref 11) have researched the pliable properties of 3104 Al amalgam subjected to DCT took after by homogenization and watched a significant change in yield quality when contrasted with basic homog-enized tests. Their work reasoned that the precipitation of second-stage particles has conferred quality because of the sticking of disengagements. DCT-treated Al-Zn-Mg-Cu compound has initiated stage change, which adjusted the microstructural mor-phology with the second-stage precipitation of Guinier-Preston (GP) zones and a metastable g¢ stage, saw through transmission electron microscopy (TEM) and first rule count (Ref 14). Thus, Al 6061 T6 subjected to DCT likewise exhibited microstructural changes which have a tendency to perform better when contrasted with industrially accessible high-quality 6xxx arrangement aluminum compounds (Ref 9, 15). In DCT, examples are absorbed a shower of strong carbon dioxide (dry ice at - 196 °C) for a stipulated timeframe. By and large, ultrafine-grained (UFG) materials are created by mechanical working which prompts extreme plastic deforma-tion. These procedures are convoluted, costly, and prompt extensive diminishment in malleability also. Consequently, the present work is focussed to enhance the mechanical properties of Al 6061 T6 by shallow cryogenic treatment (DCT), which is a moderately more affordable and basic process. The impact of Deep CT at - 196 °C for 36 h on hardness, elastic, and weakness quality of Al 6061 composite has been explored.

The hardness trial of the DCT tests were performed utilizing a microhardness analyzer. The examples for ductile tests were set up according to ASTM standard (E8M) and tried utilizing UTM. The weariness trial of DCT Al combination were performed utilizing Rotating pillar weakness testing machine, The DCT Al compound was described by utilizing XRD, optical magnifying lens, vitality dispersive x-beam spectroscopy (EDS), and SEM to explore the adjustments in stages and its morphological highlights because of DCT. The crack surface of the DCT amalgam was described by utilizing SEM-EDS to comprehend the components of change in weariness quality. The change in elasticity and weariness life of DCT Al compound was substantiated utilizing TEM and SEM-EDS comes about.

2. Experimental Procedure

The Al 6061 T6 amalgam material utilized as a part of the present examination was gotten as 25.40-mm width pole. The sythesis of the combination was acquired by optical discharge spectroscopy and announced in Table 1. The test strategy embraced in the present investigation is schematically appeared in Fig. 1. Tests were subjected to shallow CT for 36 h at 196 °C. The examples were put in a separated alumina chamber whose best was secured by cover glass fleece. The examplesweredynamicallydrenched n a strong carbon dioxide shower as demonstrated by Bensely et al. (Ref 9). The example Temperature was observed by a K write thermocouple. Since rate of cooling is a main consideration that influences the consequences of CT, the examples were gradually cooled at the rate of 0.5 °C/min, until the point when they come to the final splashing Temperature of 196 °C. A splashing time of 36 h was received to take into consideration change responses to occur. Tests were then separated and left to achieve room Temperature. Such treated examples and examples from the local material were sub-jected to metallographic examines and their mechanical properties, for example, elasticity, hardness, and weariness were estimated. The broke surfaces of the examples from the two cases were additionally examined which are accounted for in the consequent areas.

1. Micro structural Characterization

In the present examination, the examples for optical microscopy were separated from the gotten bar and one half was subjected to DCT (Fig. 2). The examples for the metallographic

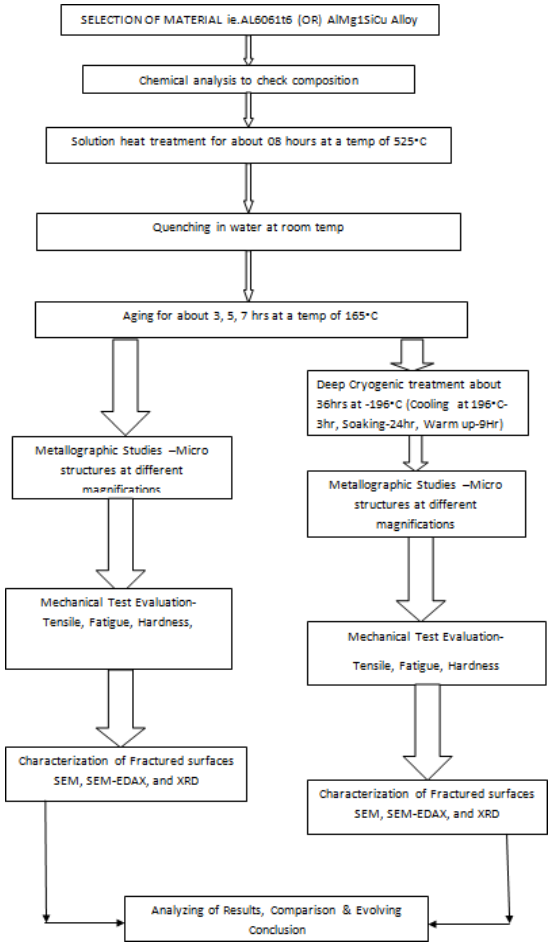

Fig. 1 Experimental procedure of the present work

Zn	Mg	Cu	Cr	Fe	Si	Mn	Ti	Al
0.044	0.992	0.290	0.250	0.128	0.627	0.028	0.205	97.696

Table 1 Percentage chemical composition of Al6061 T6

ISSN- 2394-5125 Vol 7, Issue 1, 2020

The microstructure of the examples was portrayed by an optical magnifying instrument (Carl Zeiss Axioshop arrangement). The smaller scale extension was aligned to ASTM E1951 02 prerequisites. Figure 3 and 4 look at the microstructure of the local and DCT test under various magnifications. The local examples have huge aluminum strong arrangement as network as saw from Fig. 3(a). The second-stage intermetallic particles are likewise seen in the two examples yet its sum is higher in DCT combination because of quickened precipitation at low Temperature. Figure 3(a) and 4(a) include the huge hotcake write grains with a normal grain size of 210-250 lm long and 70-110 lm in thickness bearings as estimated by the Heyn straight capture strategy (ASTM E112-12). Extremely fine accelerates are additionally found in the grain insides and grain limits.

Fig. 2 Sectioned samples for the metallographic studies

The DC-treated microstructure introduced in Fig. 3(b) and 4(b) shows uniform dispersion of the second stage, which are little flapjack write grains with a normal grain size of 60-130 lm long and 20-50 lm in thickness. The shallow CT has modified the morphology of the second stage with better dispersion in the grid composite when contrasted with untreated Al amalgam. Since recuperation is adequately smothered by the DCT treatment, the treated Al 6061 compound shows high measure of separation thickness. This prompts change in mechanical properties of polycrystalline metallic materials as announced in the writing (Ref 2). According to ASTM E112-10, the—grain estimate number expanded from 7 for the local example to 8.5 for the DC-treated example. XRD consequences of the beginning Al-6061 compound demonstrate the nearness of significant pinnacle relating to Al strong arrangement and the minor pinnacle, second-stage particles, AlMgCu, as appeared in Fig. 5(a). The DCT treatment demonstrates the nearness of Al strong arrangement and MgZn2 accelerate (Fig. 5b). TEM micrographs of local and DCT-treated examples are appeared in Fig. 6. The morphology of the grains is modified because of precipitation of second-stage particles at cryogenic gum based paint ture.

2. Evaluation of Mechanical Properties

The hardness of treated cases was evaluated by performing microhardness test using a Shimazdu MicroHard-ness Tester. The test was done after the ASTM E384-11 standard. Estimations were performed with 10N associated stack for 10 s over cleaned cases. The surface of the case was cleaned mechanically using emery paper before each HV estimation to ensure its ideal surface. Ten estimations were made at various spotlights on every illustration (both nearby and treated) and the hardness regards exhibit that SC-treated case shows higher hardness than the neighborhood case as showed up in Fig. 7. It is watched that the DCT upgraded the hardness by around 41% from 170 to 220 VHN.

Keeping in mind the end goal to comprehend the tractable properties, pliable test as indicated by ASTM E8M-13a norms was performed at encompassing Temperature. The genuine examples for the two cases are appeared in Fig. 8. Examples were machined and very much cleaned

(a) 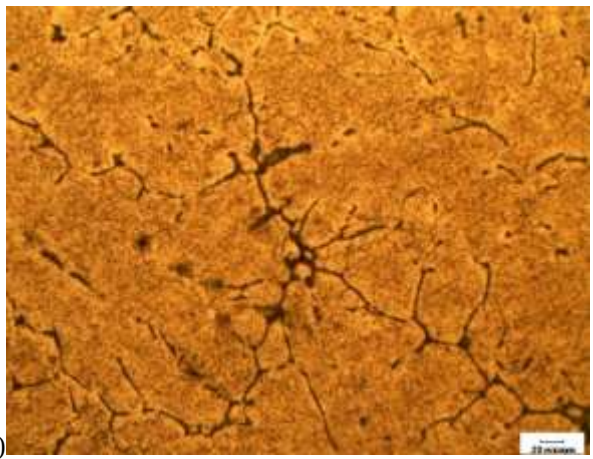 (b) 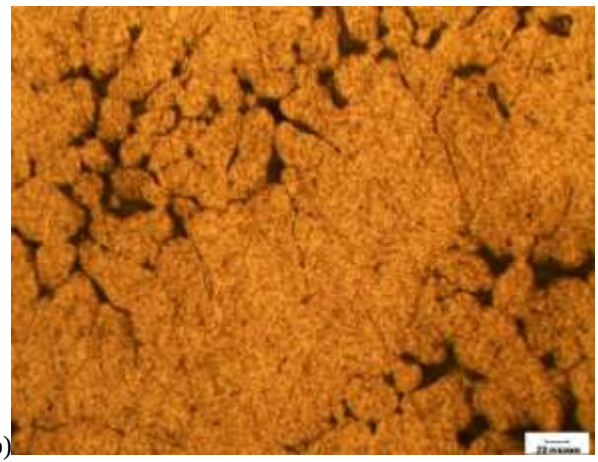

Fig. 3 Microstructure of the Al 6061 T6 alloys at 200X (a) native (b) DC-treated

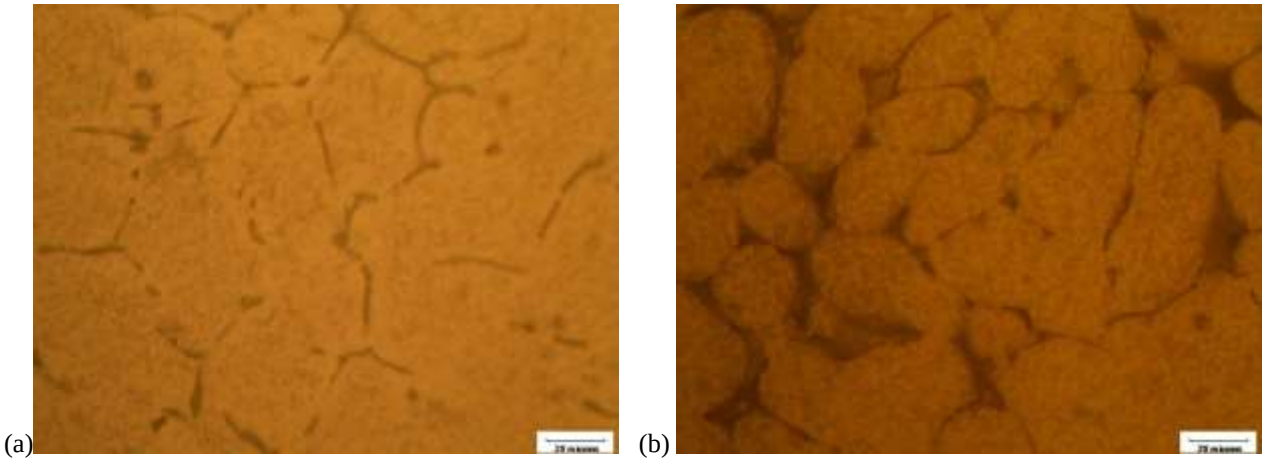

(a) (b)

Fig. 4 Microstructure of the Al 6061 T6 alloys at 500X (a) native (b) DC-treated

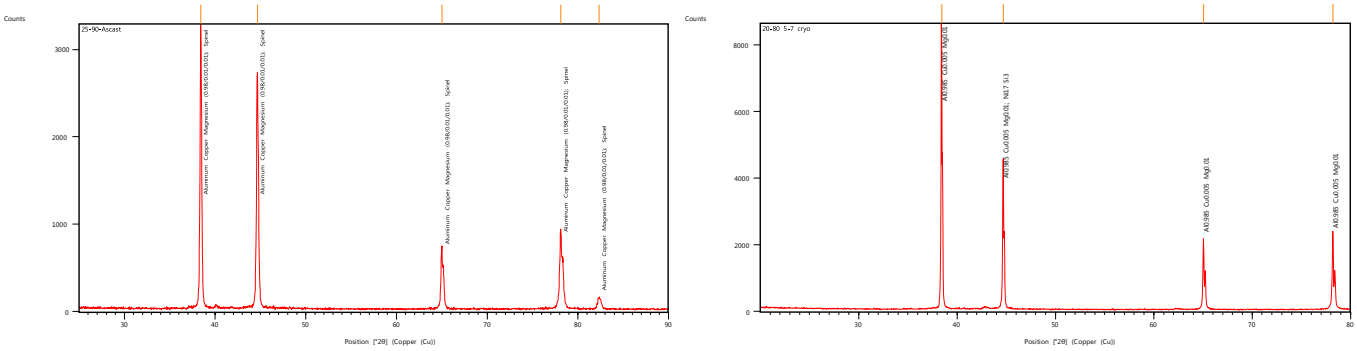

(a) (b)

Fig. 5 XRD patterns of (a) native and (b) DCT samples

with fine review emery sheet so surfaces are free of scratches. This is done to abstain from scoring impacts amid malleable stacking. It is to be noticed that the machining and cleaning were done before the treatment for the DCT tests. Four examples were tried for each situation

The aftereffects of the pliable tests are organized in Table 2 alongside the pressure strain chart appeared in Fig. 9. From Table 2, it can be watched that the UTS enhanced by around 13% from 630 to 673 MPa. Weariness quality of the DCT composite was controlled by following the ASTM E466 07. The examples were tried under pressure strain with a power controlled stacking cycle. S-N plot was acquired in light of these tests. Since split start is exceptionally touchy to microcracks in weariness tests, the examples were machined and finished with a granulating wheel. At that point, final cleaning in longitudinal bearing was accomplished utilizing 1200 work grating paper to guarantee that the example surface is free from microscratches. A servo pressure driven widespread testing load outline was utilized for weariness tests.The test frame work had a limit of ±25 kN in pivotal load, outfitted with PC control and information procurement. Every one of the tests were conducted in surrounding air. The feelings of anxiety for the weariness test were directed by the pliable test outcomes. The tests were led with R-proportions extending from 0.05 to 0.1, where R is the proportion of the base worry over the most extreme worry in a stacking cycle. At certain reasonable feelings of anxiety, the example was tried until the point that 107 stacking cycles to acquire as far as possible. Figure 10 demonstrates the S-N bend for the local and the treated examples. It can be promptly watched that at an exchanging worry of 270 MPa, the quantity of cycles to disappointment is between 1.1× 105 and 2 × 105 for the local examples, while it is between 1.4 × 106 and 1.8 × 106 for the DC-treated examples. Upon additionally testing at various feelings of anxiety, exhaustion confine is acquired at 140 MPa for the local examples as against 230 MPa for DC-treated examples. Zhao and Jiang (Ref 17) have likewise detailed a weariness cutoff of 140 MPa for the Al6061 T6. Thus, there is a change in weakness life by around

ISSN- 2394-5125 Vol 7, Issue 1, 2020

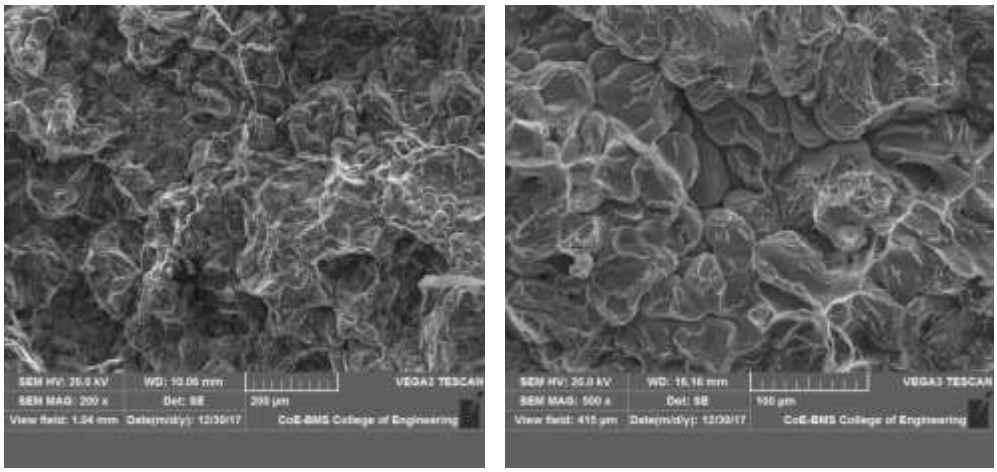

Fig. 6 SEM micrographs of (a) native (b) DCT sample

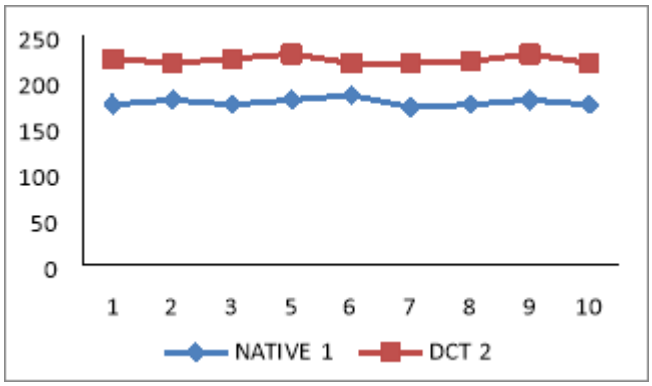

Fig. 7 Hardness profile characteristics of native and Deep Cryo-treated Al6061 T6

65%, because of the arrangement of very much appropriated second-stage particles in the DCT tests. Examples from the two cases were at first tried at 270 MPa and for the local examples, five different feelings of anxiety were endeavored to achieve as far as possible, while for the DC-treated examples, just three different levels were required to achieve as far as possible.

3. Fractography of Fatigue-Tested Samples

Since the exhaustion furthest reaches of the DC-treated example was observed to be 230 MPa, examples from the two cases were tried at 250 MPa worry to comprehend the wearinessbreak.

break surfaces of weariness tried examples from the two cases were analyzed under TEM and fractographs were gotten. Three phases in the life of a weariness disappointment, for example, start, break development (engendering), and final crack were identified and talked about underneath. The bolt in Fig. 11 demonstrates the split start point for both the cases showing that the break starts from the surface. Figure 12(a) demonstrates the break surface of the local example with dimple burst. Figure 12(b) demonstrates the crack surface of the SC-treated example with dimple break causing the bendable crack. The development of dimpled surface demonstrates the pliable kind of break in the tried examples. The event of pliable method of break is because of the development and mixture of microvoids when the example is subjected to exhaustion stack (Ref 19, 20). The accelerate particles get isolates from the encompassing framework due to triaxial condition of pressure and structures microvoids, which along these lines develops in measure under powerful load, and show up as dimpled surface. It is to be noticed that the fibrous structure is held in the treated example prompting little change in pliability. Figure 12(c) demonstrates the weariness striations of the local example. An expanded perspective of the striations is displayed in Fig. 12(d). Essentially, the striations in the treated example and its comparing expanded view are seen from Fig. 12(e) and (f). It can be watched that the striations are denser in the treated example contrasted with the local example advocating the expansion in weariness quality in the treated example.

4. EDS Analysis

EDS pinnacles of local and treated examples are appeared in Fig. 13(a) and (c), individually. The zones in which EDS was

ISSN- 2394-5125 Vol 7, Issue 1, 2020

(a) (b)

Fig. 8 (a) Native samples (b) Deep cryogenic-treated samples

Table 2 Tensile test results

Conditions	Specimen code	Yield strength, MPa	Average, MPa	Tensile strength, MPa	Average, MPa	% Elongation	Average, %
Native material	A	430	432	440	530	9.14	
	B	426		432		8.94	
	C	434		420		9.20	
	D	439		428		10.16	9.11
DCT	A	522	520	580	573	7.05	6.85
	B	514		565		6.86	
	C	521		568		6.94	
	D	520		576		6.56	

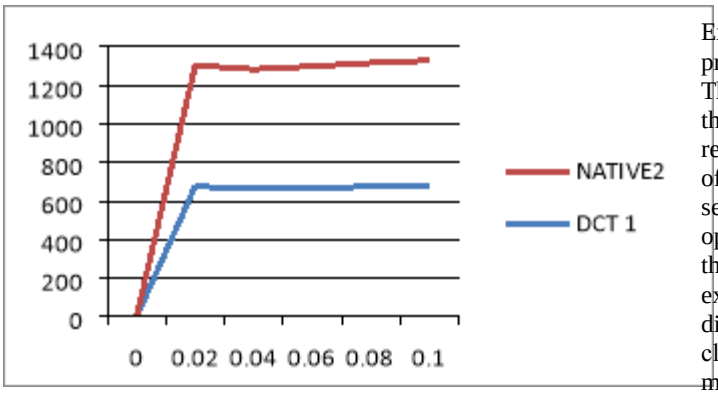

Fig. 9 Stress-strain characteristics of native and DCT Al6061 T6

performed are seen from Fig. 13(b) and (d). The Mg-rich (MgZnCu) stages were insignificant in the DCT test demonstrating that they were totally broken down in the framework amid the DCT. The return of MgZn2 accelerates in DCT material demonstrates the basic adjustments and the precipitation of second-stage particles because of supersaturated strong arrangement state came to at low Temperature (80 °C). The disengagement thickness in the combination has expanded at cryogenic Temperature because of concealment of recuperation.

5. Discussion

Examination of the DCT composite has demonstrated the precipitation of MgZn2 particles as clear from Fig. 3(b) and 4(b). The quality of the SC-treated Al 6061 combination is higher than the T6 proportionate showing that it is conceivable to build the reinforcing impact through the DCT procedure. The high quality of DCT composite might be ascribed to precipitation and high separation thickness. Examinations on the pictures acquired from optical magnifying instrument and TEM appear (Fig. 3, 4, and 13) that thickness of separations has expanded in the SC-treated example, which gives high quality to the amalgam because of disengagement solidifying. The high thickness of disengagement close to the grain limits makes it difficult for the separation to move starting with one slip plane then onto the next slip plane. The nanosized fine accelerates impede simple separation float. Thus, the dislo-cations dodge the encourages and it has a tendency to amass more because of Frank-Read source components, granting higher quality to the DCT amalgam. Thus, the hastens assume an imperative part in expanding the quality because of Zener drag impact. It is to be noticed that the accelerates and separations together increment the quality of the treated amalgam. A comparable perception is made by Zhang et al. (Ref 11) and they revealed that the GP zones are less in the treated examples.

The enhanced exhaustion life and continuance restrict were seen if there should be an occurrence of DCT-regarded Al 6061 amalgam when contrasted with local compound because of the precipitation ofsecond-stage

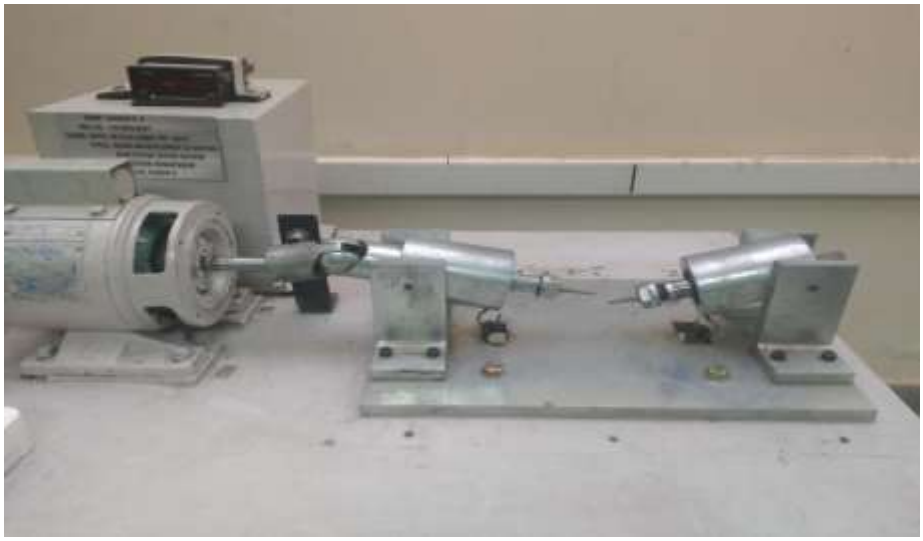

Fig. 10 fatigue test apparatus for the native and DCT-treated samples

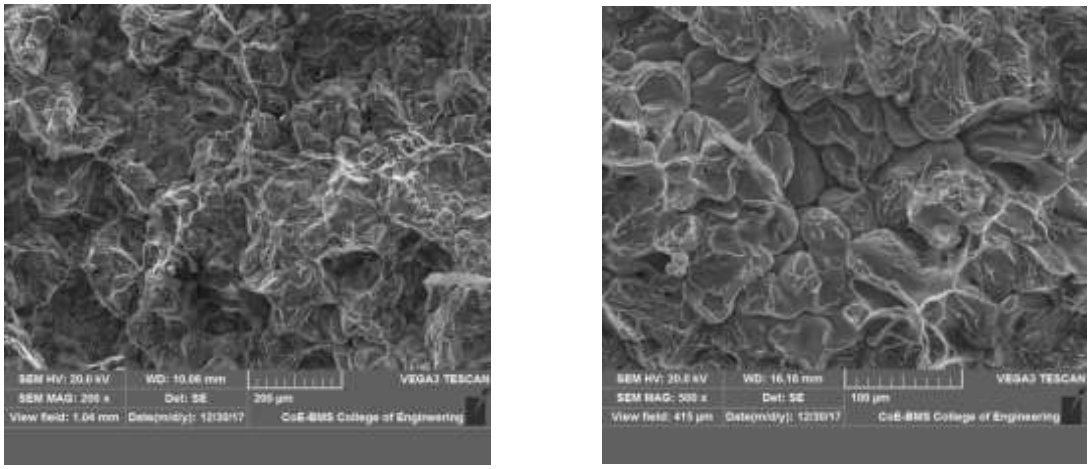

(a) (b)

Fig. 11 SEM images of fatigue-fractured surface. Crack initiation from the surface (a) native (b) DCT sample

particles. SEM portrayal of the examples broke under weakness stacking has been completed to uncover the change in break morphology from the high to low pressure locale. An all around refined morphology and better appropriation of second-stage particles could back off the split proliferation rate in the DCT Al composite. Watchful investigation by SEM over a wide region demonstrated that some sub-grains of 2-5 lm in distance across can be seen in the microstructure of beginning material. The mean grain size of the underlying microstructure ascertained by region portion technique is around 9 lm, though the mean grain size of the SC-treated microstructure figured by region part strategy is about 3.5 lm. The sub-grain structures are relied upon to frame pre-overwhelmingly from the revamp of basic separations upon DCT treatment. The collaboration between second-stage particles and prior separation may influence the development of high disengagement thickness, which thusly could contribute for the arrangement of sub-grains in the composite. Portrayal at higher magnification by SEM (Fig. 14) demonstrates the nearness of encourages in local and DCT Al 6061 T6 examples. The expansive plate-like hastens relate to MgZn2 stage as obvious from EDS comes about. The disengagements are found in the local example yet separation thickness is high in the DCT test because of concealment of recuperation. The morphology of the treated and locals tests is appeared in SEM micrographs, (Fig. 6). The refinement of morphology in the regarded test is apparent when contrasted with the local example because of adjustment and precipitation of second-stage particles. The supersaturated strong arrangement state came to at cryogenic Temperature could modify andencouragequick

ISSN- 2394-5125 Vol 7, Issue 1, 2020

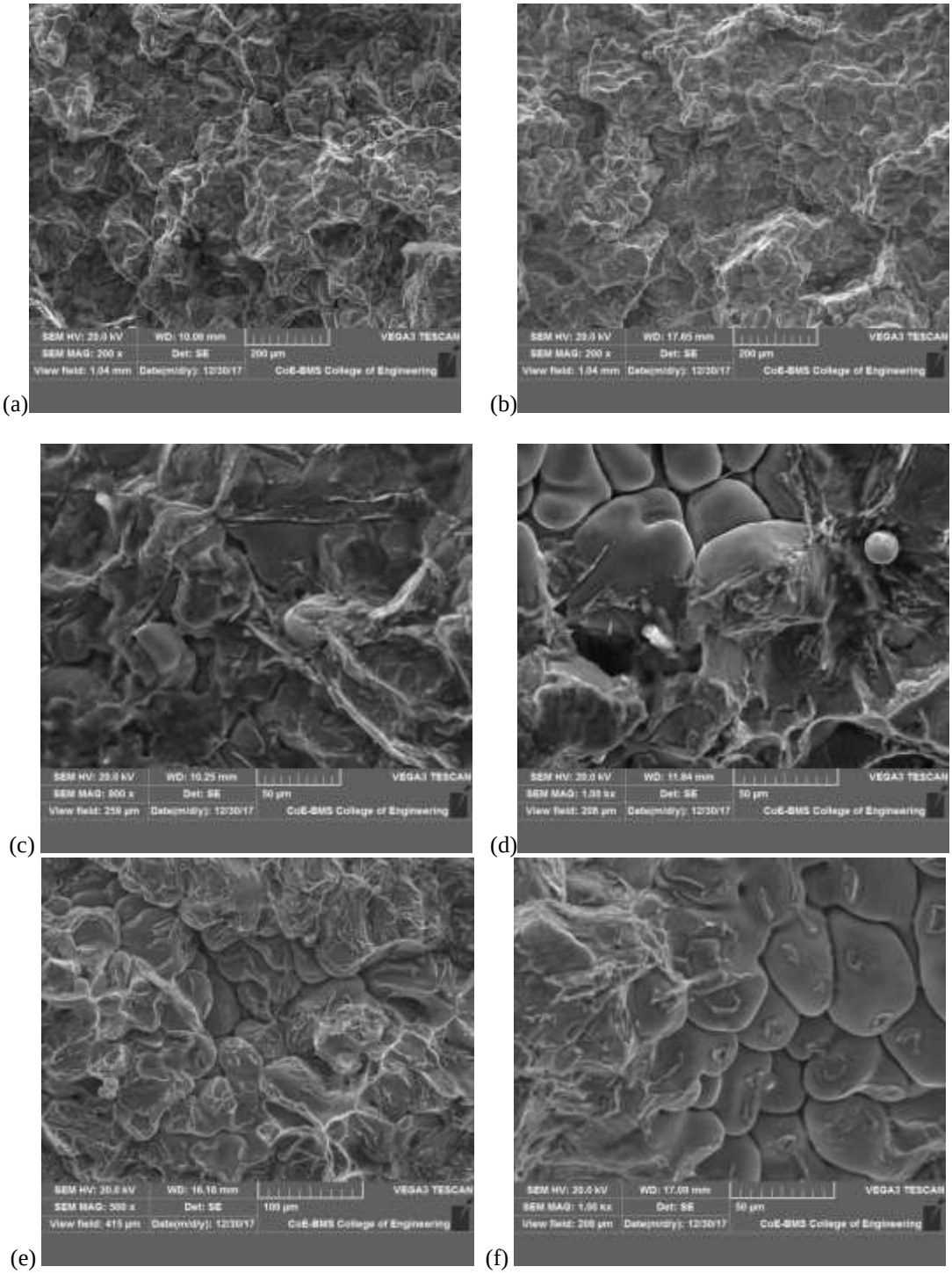

Fig. 12 SEM images of fatigue fracture surface. Dimple ruptures (a) native (b) DCT sample. Fatigue striations in the crack propagation zone (c) native (d) native at a higher magnification (e) DCT sample (f) DCT sample at a higher magnification

arrangement of groups from GP zones, from which hastens rise out effortlessly (Ref 14). A point by point HRSEM examination is important to render encourage knowledge into the bunch development and its influence on precipitation. Prior reports by Park and Ardell (Ref 16, 17) and Gjonnes and Simensens (Ref 18) have portrayed that microstructure of Al-6061 composite through the crest matured (T6) hardening condition contains dominatingly g progress stage. A little measure of GP zones may likewise be available in the combination, which requires SEM examination for discovery. Additionally, it might be finished up from the EDS comes about (Fig. 13) that both GP zones and g stage are found in the T6 examples and for the DCT combination.

ISSN- 2394-5125 Vol 7, Issue 1, 2020

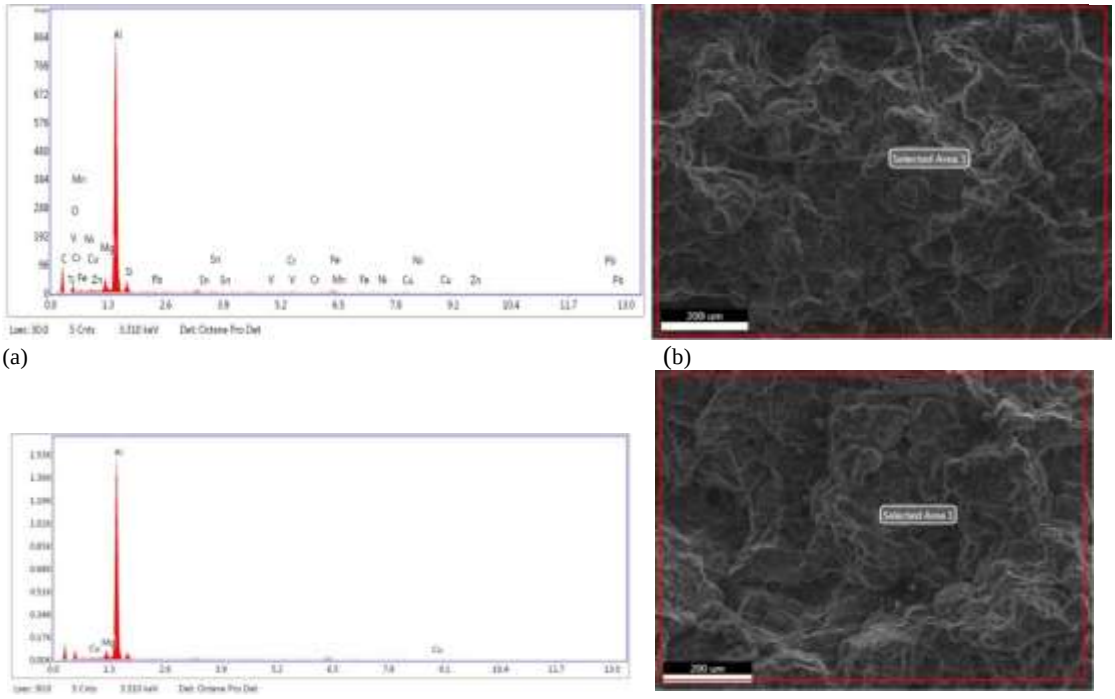

(a) (b)

(c) (d)

Fig. 13 (a) EDS pattern of native sample (b) Sample location of EDS spot (c) EDS pattern of DCT sample (d) Sample location of EDS spot

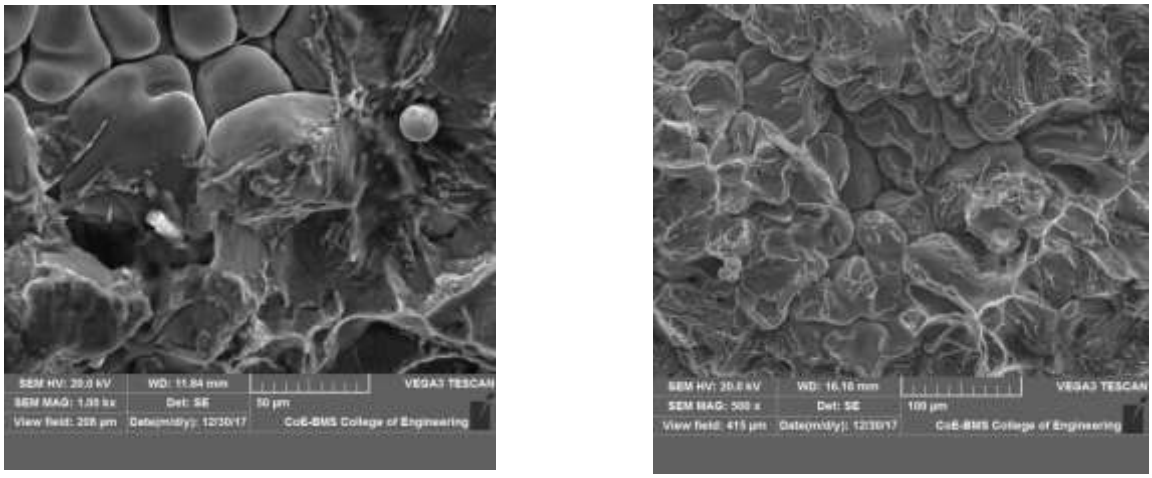

(a) (b)

Fig. 14 (a) SEM image of native sample (b) SEM image of DCT sample

6. Conclusions

The present work examined the impact of DCT on the mechanical properties of Al 6061 compound and the iSEMized microstructural portrayal of DCT amalgam was made utilizing optical, SEM/SEM, EDS, and SEM. The accompanying conclusions are made in view of the present examination.

•The DCT Al amalgam has indicated refined microstructural morphologies when contrasted with the local composite as obvious from

optical and SEM micrographs. Particularly, the hasten particles are consistently diseminated and its size has diminished because of CT.

•The development of encourages has been quickened for the DCT Al combination because of the adjustment of point deformities and separations and in addition the supersaturated strong solu-tion state achieved upon delayed presentation to cryogenic conditions.

•SEM and SEM-EDS comes about have confirmed the improvement of microstructural morphologies, bringing about the refined second-stage particles when contrasted with local example.

•Mechanical testing of DCT composite has demonstrated that an in-wrinkle of 20% in yield quality, 30% in hardness, 10% in UTS, 64% in weakness restrict and an abaSEMent of 22% in elon-gation. The change in yield quality is because of the aggregated separation thickness and encourages in the DCT combination, which prompted diminishment in extension according to Hall-Petch impact.

•The change in weariness quality of DCT Al composite is because of uniform conveyance of second-stage particles, which im-pedes split development viably due its fine morphology. Higher separation thickness in the DCT composite could likewise re-strict split development as it separates the coherence of the slip plane from one grain to the nearby grain.

•DCT is a less expensive process contrasted with DCT and it im-separated considerable change in elastic (630 to 673 MPa) and weariness properties of Al compound (from 140 to 240 MPa) as clear from the present work.

References

1. S. Jia, D. Zhang, and L. Nastac, Experimental and Numerical Analysis of the 6061-Based Nanocomposites Fabricated Via Ultrasonic Pro- cessing, *J. Mater. Eng. Perform.*, 2015, 24(6), p 2225–2233
2. J. Gjønnes and C.J. Simensen, The Precipitate, *Acta Metall.*, 1970, 18, p 881–890
3. J.K. Park and A.J. Ardell, Precipitate Microstructure of Peak-Aged 6061 Al, *Scr. Metall.*, 1988, 22, p 1115–1119. doi: 10.1016/S0036-9748(88)80114-5
4. H. Panchakshari, D. Girish, and M. Krishn, Effect of Deep Cryogenic Treatment on, Microstructure, Mechanical and Fracture Properties of Aluminium-Al 203 Metal Matrix Composites, *Int. J. Soft Comput. Eng.*, 2012, 1(340), p 340–346
5. J.K. Park and A.J. Ardell, Microstructures of the Commercial 6061 Al Alloy in the T651 and T7 TEMpers, *Metall. Trans. A*, 1983, 14, p 1957– 1965. doi:10.1007/BF02662363
6. C. Li, N. Cheng, Z. Chen, N. Guo, and S. Zeng, Deep-Cryogenic-Treatment-Induced Phase Transformation in the Al-Zn-Mg-Cu Alloy, *Int. J. Miner. Metall. Mater.*, 2015, 22, p 68–77. doi: 10.1007/s12613-015-1045-7
7. F. Bouzada, M. Cabeza, P. Merino, and S. Trillo, Effect of Deep Cryogenic Treatment on the Microstructure of an Aerospace Aluminum Alloy, *Adv. Mater. Res.*, 2012, 445, p 965–970
8. W. Zhang, P. Bai, J. Yang, H. Xu, J. Dang, and Z. Du, Tensile Behavior of 3104 Aluminum Alloy Processed by Homogenization and Cryo- genic Treatment, *Trans. Nonferrous Metals Soc. China*, 2014, 24(8), p 2453–2458. doi:10.1016/S1003-6326(14)63370-7
9. P. Das, R. Jayaganthan, T. Chowdhury, and I.V. Singh, Fatigue Behaviour and Crack Growth Rate of Cryorolled Al 6061 Alloy, *Mater. Sci. Eng. A*, 2011, 528, p 7124–7132. doi:10.1016/j.msea.2011.05.021
10. P. Baldissera, Deep Cryogenic Treatment of AISI, 302 Stainless Steel: Part I—Hardness and Tensile Properties, *Mater. Des.*, 2010, 31, p 4725–4730. doi:10.1016/j.matdes.2010.05.013
11. A. Bensely, D. Senthilkumar, D. Mohan Lal, G. Nagarajan, and A. Rajadurai, Effect of Cryogenic Treatment on Tensile Behavior of Case Carburized Steel-815M17, *Mater. Charact.*, 2007, 58, p 485–491. doi: 10.1016/j.matchar.2006.06.019
12. P. Chen, T. Malone, R. Bond, and P. Torres, Effects of Cryogenic Treatment on the Residual Stress and Mechanical Properties of an Aerospace Aluminum Alloy, *Proc. 4th Conf. Aerosp. Mater. Process. Environ. Technol.*, 2001
13. J. Liu, G. Li, D. Chen, and Z. Chen, Effect of Cryogenic Treatment on Deformation Behavior of As-Cast az91Mg Alloy, *Chin. J. Aeronaut.*, 2012, 25, p 931–936. doi:10.1016/S1000-9361(11)60464-0
14. P. Baldissera and C. Delprete, Deep Cryogenic Treatment: A Bibliographic Review, *Open Mech. Eng. J.*, 2008, 2, p 1–11. doi: 10.2174/1874155X00802010001
15. K.E. Lulay, K. Khan, and D. Chaaya, The Effect of Cryogenic Treatments on 6061 Aluminum Alloy, *J. Mater. Eng. Perform.*, 2002, 11, p 479–480. doi:10.1361/105994902770343683
16. N. Mahathaninwong, T. Plookphol, J. Wannasin, and S. Wisutmethangoon, T6 Heat Treatment of Rheocasting 6061 Al Alloy, *Mater. Sci. Eng. A*, 2012, 532, p 91–99. doi:10.1016/j.msea.2011.10.068
17. R. Smallman and A. Ngan, Physical Metallurgy and Advanced Materials, Vasa, 2011
18. J.C. Williams and E.A. Starke, Progress in Structural Materials for Aerospace SysTEMs, *Acta Mater.*, 2003, 51, p 5775–5799. doi: 10.1016/j.actamat.2003.08.023